Changes in Cement Mass under the Influence of Consciousness Bond Field: A Study of Taheri Consciousness Theory

Bahareh Kazazi [1*], Mohammad Ali Taheri [2]

1. Civil Engineering, CEO of Hoobe Construction Company, Tehran, Iran.

2. Sciencefact R&D Department, Cosmointel Inc. Research Center, Ontario, Canada.

* Corresponding author:

Bahareh Kazazi
Civil Engineering, CEO of Hoobe Construction Company, Tehran, Iran.

Email: baharkazazi@gmail.com

The First Journal in T-Consciousness Research
Journal of Cosmo Intel
36

ABSTRACT

Taheri Consciousness (T-Consciousness) was introduced and defined by Mohammad Ali Taheri as one of the constituent components of the Cosmos in addition to matter and energy, from which Taheri Consciousness Fields (TCFs) are derived. TCFs are not matter or energy, but they can be proven by scientific experiments. In this regard, extensive research on materials indicates that the occurred changes require energy. As no energy was applied during the experiment, the only reason for these changes was the existence of T-Consciousness. By examining the behavior of cement in various functions, it was found that in many cases, the water absorption of cement was reduced or remained constant while the number of elements had changed. This finding raised the possibility of a change in the mass of the matter. This study investigated the volume and mass of 9 identical cement samples up to 28 days old. It was found that water absorption under T-Consciousness Field was still lower (-2.8%, -2.6%), the mass of the samples increased (3 to 4%), and the percentage of crystalline phase was higher in the samples under the Field. TGA (Thermal gravimetric analysis), DTA (Differential thermal analysis), and DSC (Differential scanning calorimetry) analysis results were consistent with XRF (X-Ray Fluorescence) and XRD (X-ray Diffraction).

Keywords: Consciousness Bond Field, Taheri Consciousness Fields, Crystal changes, Cement, Mass change, Thermal analysis

INTRODUCTION

Throughout history, humans have been curious about the world around them. Many efforts have been made in this direction, leading to the discovery of many principles, laws, and fields, such as gravitational field, electromagnetic field, electric field, etc.

The nature of consciousness and its place in science has received much attention in the current century. Many philosophical and scientific theories have been proposed in this area. In the 1980s, Mohammad Ali Taheri introduced novel fields with a non-material/non-energetic nature named Taheri Consciousness Fields (TCFs). In this perspective, T-Consciousness is one of the three existing elements of the universe apart from matter and energy and can be converted into matter and energy and vice versa [1,2].

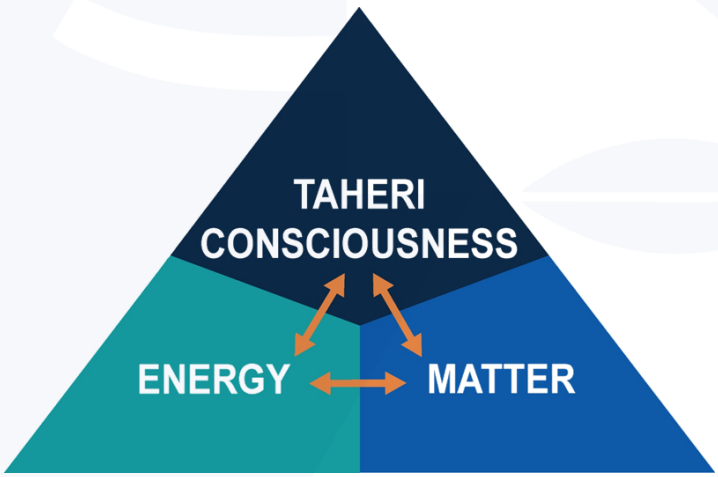

Figure 1. The relationship between T-Consciousness, matter, and energy in the theory of TCFs

According to this theory, there are various TCFs with different functions, which are the subcategories of a networked universal internet called the Cosmic Consciousness Network (CCN). The major difference between the theory of TCFs and other theoretical concepts about consciousness is related to the practical application of the TCFs. TCFs can be applied to all living and non-living creatures, including plants, animals, microorganisms, materials, etc.

Mohammad Ali Taheri, the founder of Erfan Keyhani Halqeh, a school of thought, introduced a new science in 2020 as a branch of this school. He coined the term Sciencefact for this new science because it utilizes scientific investigations to prove the existence of T-Consciousness as an irrefutable phenomenon and a fact. Although science focuses solely on the study of matter and energy and Sciencefact, by contrast, explores the effects of the [non-material/non-energetic] TCFs, Sciencefact has provided a common ground between the two by conducting reproducible laboratory experiments in various scientific fields, and it has used the scientific approach in proving TCFs.

The influence of the TCFs begins with the Connection between CCN as the Whole Taheri Consciousness of the universe and the subjects of study as a part. This Connection called "Ettesal" is established by a certified and trained individual who has been entrusted

with the TCFs. The human mind has an intermediary role (Announcer) which plays a part by fleeting attention to the subject of study and then the main achievement obtained as a result of the effects of the TCFs. These Fields cannot be directly measured by science, but it is possible to investigate their effects on various subjects through reproducible laboratory experiments.

The research methodology in the study of T-Consciousness has been founded on the process of Assumption, Argument, and Proof, in which the basic Assumption is: The Cosmos was formed by a third element called T-Consciousness that is different from matter and energy.

The Argument: The existence of TCFs can be demonstrated by their effects on matter and energy (e.g., humans, animals, plants, microorganisms, cells, materials, etc.)

The Proof: is the scientific verification of the effects of TCFs on matter and energy (according to the Argument) through various reproducible scientific experiments.

Accordingly, to investigate and verify the existence, effects, and mechanisms of TCFs, the following five research phases (Phases 0 through 4), and the aims of each phase are outlined below.

Phase-0 studies aim to prove the existence of TCFs by observing their effects. The nature of T-Consciousness and what it is will not be addressed in this phase. Phase-1 explores the varied effects of different TCFs. Phase-2 examines the reason behind the varied effects of these fields. Phase-3 investigates the mechanism of TCFs effects on matter and energy. Finally, Phase-4 draws significant conclusions, particularly with regard to the mind and memory of matter and their relation to the T-Consciousness, etc. [1, 2,3]

Research on the function and behavior of materials under the influence of TCFs began a decade ago. In one study, the crystal defects in two methods were examined. The findings indicated that the crystal reached by casting pure 1000 series aluminum from a single ingot at ambient temperature, increased the mold volume, and applying 300 ° C preheating, had higher growth in the internal defects, up to 1000% in some cases [4,5]. As we know, the formation of defects requires the transfer of energy, which is mainly provided in the form of mechanical thermal behavior, by creating external stress for the material [6]. In these samples, as the material, energy-based factors were constant, the only influential factor must be something beyond energy and material, which according to Taheri it is the third element of the universe; T-Consciousness. The previous study revealed that TCFs had significant effects on lattice irregularities [4,5]. As we can see, creating this level of displacement requires an energy supply [6].

In the previous dilatometric study on the 99.9% pure copper, we examined the samples of the same length, under the same conditions and heated them up to 300 ° C. Compared with the samples under the T-Consciousness Field, relative increases in the length of the control samples were reported. Also, a reverse trend of density changes was identified in the samples under T-Consciousness Field compared with controls [7].

Moreover, in a repeated experiment, the mechanical crushing of pure silica samples was tested to measure its properties. The application of mechanical force simultaneously under the same conditions, and using the same device created the same silica powder, which was 80% lower than the average micro-strain of the crystal lattice [8,9]. This decrease indicated that the internal stresses in the crystal structure of the samples were significantly reduced, and the obtained crystalline structures had very little lattice distor-

tion. This finding indicated that despite the application of external force, the samples under the T-Consciousness Field were still much more able to keep the structure of their crystal lattice without distortion compared to the control.

Continuation of the research over the years has resulted in the examination of many pieces of cement made according to international standards under the influence of TCFs. The aim of previous research was to investigate the overall function and behavior of concrete and cement mortar in increasing strength, concrete cancer, penetration of chloride ions, bending of concrete beams, penetration of gamma-newer radiation, and some other factors. However, in this study, the process of internal change revealed many points about how T-Consciousness Fields influences materials. Among the points is that in XRF (X-Ray Fluorescence) analysis, in addition to changing the water content percentage of the samples, the weight percentage of the elements of the samples had parallel changes [10-13].

In fact, in the XRF test, a part of the sample is first weighed and then placed in a furnace and heated to 1100 ° C for 2 hours, then weighed again and the percentage of weight loss due to heat is reported by LOI (Loss on Ignition).

Given that the total percentage of all phases along with the value (Loss on Ignition) of LOI should be equal to 100, increasing or decreasing the percentage (Loss on Ignition) of LOI causes the percentage of other phases to change. However, a significant point was observed in all cases, i.e., sometimes with the report of less or equal water absorption, extensive, purposeful, and reproducible changes have been made in the type and number of elements.

Studying the changes in the strength of cement samples on the 90th day, although these samples were made with the standard sand and the LOI average ± 1% LOI was the same in the experimental and control samples, the percentage of elements had changed. It makes it more probable that these changes lead to mass change, particularly since the calcium element constitutes more than 60% by weight of cement and in some cases has shown 13% changes [10]. Obviously, T-Consciousness affected the chemical composition and function of matter, and the fundamental question was whether these changes led to a change in mass in the samples.

Materials and methods

Analyses

For the first stage, a random bag of cement was selected. In order to analyze the chemical and elemental properties of the sample, XRF analysis was carried out. Then 9 cement samples with the Normal concentration were prepared according to the ASTM C187 standard and were categorized, and labeled into three groups of three by the laboratory official (Figure 2)

One group was identified as the control group (OPC), and two groups were selected as the experimental groups to be examined under the influence of TCFs 1 and 2 (different TCFs) labeled as N and M, respectively. The dimensions and mass of all samples were measured on the first, seventh, fourteenth, and twenty-eight days using a scale. On the 28th day, XRF and XRD (X-ray Diffraction) tests, a technique for analyzing the cement's crystal structures, were done on all samples in the same instrument, under the same conditions, and with the same amount of material.

All cement samples were pulverized by the laboratory prior to analysis (Figure 3).

Due to the similarity of the results of the trend changes, the second sample NO.2 of each group was selected and examined more thoroughly, and the following thermal analysis tests were carried out. In the analysis, the mass amount of all samples was 6 mg and the temperature growth rate was 10 °C, in the temperature range of 25 to 1000 °C, by ASTM-E1131 and was in the American (TA): SDT Q600 V20.9 Build20, in Air, with the following specifications: Three thermal analyses of TGA (Thermal Gravimetric Analysis), DTA (Differential Thermal Analysis), and DSC (Differential Scanning Calorimetry) were carried out to quantitatively examine the compounds present in these samples.

Before starting the main experiment, the weight percentage of elements and the water adsorption of the dry powder cement used in this research were measured. The details are presented in Table 1: A small amount of LOI (≈1.7%) in the untreated sample indicates the existence of the heat-resistant ceramic structures, and a minimal amount of these structures have been decomposed by heat.

Table 1. Results of XRF test related to cement before hydration

Na_2O%	0.11	MgO%	1.7	$Al_2O_{3\%}$	2.22	$SiO_{2\%}$	19.5	$SO_{3\%}$	2.8
K_2O%	0.66	CaO%	66.0	$TiO_{2\%}$	0.35	$Fe_2O_{3\%}$	5.0	L.O.I%	1.66

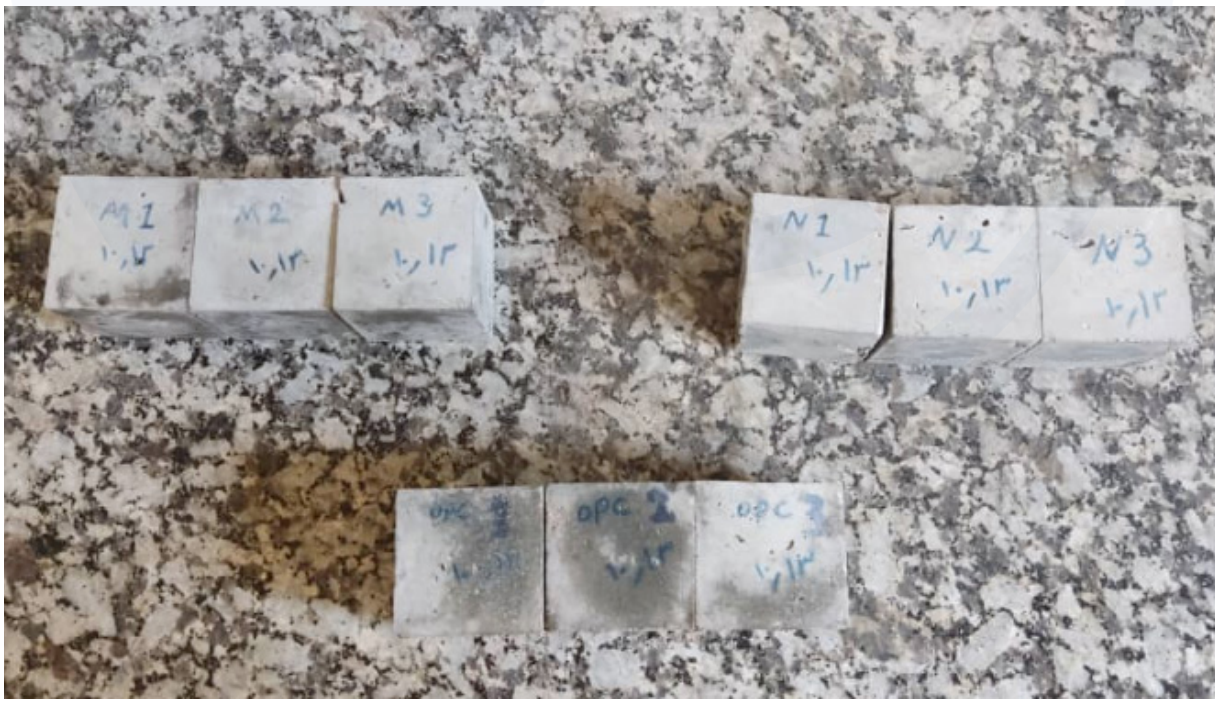

Figure 2. The Cement samples

Figure 3. The Powder Cement samples NO.2 of each sample after hydration. Samples from right to left, respectively: Control2, M2, N2

Application of the Taheri Consciousness Field

One of the TCFs, called the Consciousness Bond Field, was applied to the samples according to the protocols regulated by the COSMOintel research center (www.COSMOintel.com). A request for Connection to the CCN to utilize TCFs can be placed through the COSMOintel website in the "Assign Announcement" section. This access is available for everyone at no cost. In order to study and experience this Connection, the researchers can register on the website at any time in order to report the experiment to the COSMOintel research center. Certain details of the experiment must be provided to the center; for example, the characteristics or number and name of samples and controls must be specified. This entire experiment was carried out as a double-blind method where lab technicians were completely unaware of the TCFs theory, and the *Announcer* at the COSMOintel research center who established the Connection was unaware of the details of the study. Double-blind is a gold standard common in science experiments.

Results and discussion

Changes in the dimensions and mass of the cement samples up to 28 days of age are collected in tables 2 and 3. Table 4 summarizes the comparison of the groups for the days 7,14,28.

Table 2 . Changes in the dimensions of the samples up to 28 days of age

Groups	Samples	1-day(cm)	7-day(cm)	14-day(cm)	28-day(cm)
The OPC Control	OPC1	5.05×5.00×5.25	5.05×5.00×5.25	5.05×5.00×5.25	5.05×5.00×5.25
	OPC2	5.18×5.00×5.07	5.18×5.00×5.07	5.18×5.00×5.07	5.18×5.00×5.07
	OPC3	5.20×5.00×5.00	5.20×5.00×5.00	5.20×5.00×5.00	5.20×5.00×5.00
N (TCF1)	N1	5.10×5.00×5.18	5.10×5.00×5.18	5.10×5.00×5.18	5.10×5.00×5.18
	N2	5.24×5.13×5.02	5.24×5.13×5.02	5.24×5.13×5.02	5.24×5.13×5.02
	N3	5.25×5.10×5.00	5.25×5.10×5.00	5.25×5.10×5.00	5.25×5.10×5.00
M(TCF2)	M1	5.15×5.05×5.00	5.15×5.05×5.00	5.15×5.05×5.00	5.15×5.05×5.00
	M2	5.18×5.05×5.00	5.18×5.05×5.00	5.18×5.05×5.00	5.18×5.05×5.00
	M3	5.00×5.10×5.24	5.00×5.10×5.24	5.00×5.10×5.24	5.00×5.10×5.24

Table 3 . Mass changes of the cement samples up to 28 days of age

Groups	Samples	1-day (gr)	Mean	7-day (gr)	Mean	14-day (gr)	Mean	28-day (gr)	Mean
OPC Control	OPC1	285.50		287.06		287.97		288.62	
	OPC2	276.90	277.93	282.69	281.71	283.56	284.51	284.21	285.15
	OPC3	275.40		275.4		282.01		282.64	
N(TCF1)	N1	274.44		280.32		281.32		281.93	
	N2	285.92	280.90	291.60	286.74	292.66	287.76	293.25	288.36
	N3	282.35		288.3		289.31		289.92	
M(TCF2)	M1	271.39		277.27		278.25		278.83	
	M2	278.13	276.01	284.18	281.85	285.2	282.85	285.76	283.46
	M3	278.51		284.12		285.11		285.72	

Table 4 . Mean mass changes compared to the first day and percentage change compared to the control

Groups	7-day	14-day	28-day
OPC-control	3.78	6.58	7.22
N-TCF1	5.84	6.86	7.46
M-TCF2	5.84	6.84	7.45
Changes%	56%	4.3%	3.3%

Considering that the N samples had an average of about 1% higher mass on the first day, it is obvious that the mold volume was larger by an average of 3 mm^3. As the average of the three M samples had 0.6% less mass than the control sample, it can be said that at 28 days of age, the samples exposed to TCF2 have a higher mass increase rate of about 3 to 4% compared to the controls. Since the samples are kept in water until the age of 28 days, one of the reasons for this increase could be higher water absorption. For this purpose, the Loss on Ignition (LOI) test was carried.

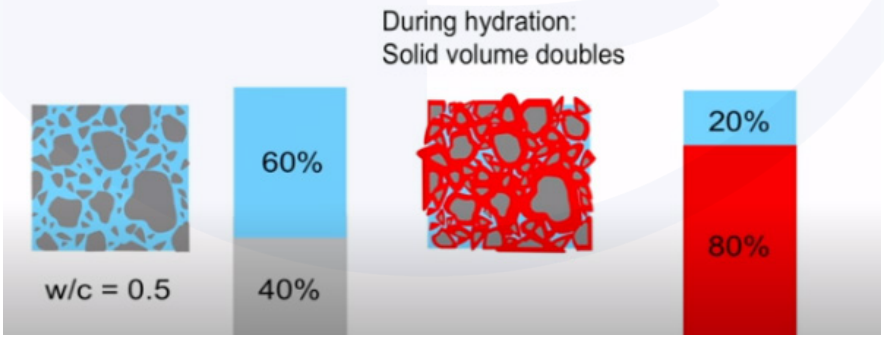

Figure 4. Schematic illustration of cement hardening

XRF (X-Ray Fluorescence) analysis

During the XRF test, part of the sample is first weighed and then placed in a furnace and heated to 1100 ° C for 2 hours, then weighed again and the percentage of weight loss due to heat is reported by LOI (Loss on Ignition).

Table 5 . XRF test of weight percentage of elements and water absorption LOI

Name		Control			TCF1			TCF2	
OXID%	OPC1	OPC2	OPC3	N1	N2	N3	M1	M2	M3
Na2O	0.07	0.07	0.05	0.05	0.09	0.07	-	-	-
MgO	1.5	1.51	1.5	1.3	1.5	1.5	1.2	1.2	1.1
AL_2O_3	2.14	1.9	1.9	1.8	1.9	1.9	1.43	1.67	1.6
SiO_2	15.2	14.9	14.9	15.1	15.7	15.6	15.2	14.9	13.4
P_2O_5	0.08	0.08	0.09	0.1	0.09	0.09	0.16	0.19	0.21
SO_3	1.9	1.6	1.6	1.5	1.5	1.6	1.7	1.5	1.7
K_2O	0.56	0.58	0.56	0.53	0.56	0.60	0.6	0.567	0.56
CaO	51.7	52.6	52.5	50.5	52.1	52.3	52.6	53.6	54.6
TiO_2	0.27	0.28	0.27	0.26	0.27	0.27	0.32	0.31	0.31
Fe_2O_3	3.5	3.3	3.4	3.3	3.4	3.3	3.8	3.4	3.5
LOI	23.08	23.18	23.23	22.56	22.89	22.07	22.09	22.66	22.97
Average LOI		**23.16**			**22.5**			**22.5**	

Table 6 . The average weight percentage of some elements obtained after heat loss and the percentage change in them compared to the control

Name	Na	%	Mg	%	AL	%	Ca	%	P	%	Ti	%	LOI	%
OPC	0.06	*	1.5		1.98		52.26		0.08		0.27		23.16	
N(TCF1)	0.07	-	1.4	-6	1.86	-6	51.63	-1	0.09	12.5	0.27		22.5	-2.8
M(TCF2)	-	100%	1.1	-26.6	1.56	-15	53.6	2.5	0.18	125	0.31	14.8	22.57	-2.6

The LOIs show that sample M and sample N have lost less weight of water on average 2.6% and 2.8%, respectively. That is, the wa-ter absorption of the samples is less than the control. Therefore, the mass of 3 to 4% is not more dependent on the water absorption.

The Results of the XRD (X-Ray Diffraction)

XRD test was used to investigate the crystal structures in the three samples of processed cement. The diffraction patterns are provided below. It should be noted that the following data include two parts: qualitative (phase identification) and quantitative (amount of compounds). The quantitative part can only be used as a reference point for the general understanding, and other well-known methods should be used if you want to examine the quantitative.

Raw Data Origin: XRD measurement (*.XRDML)
Start Position [°2Th.]: 3.0011
End Position [°2Th.]: 79.9091
Step Size [°2Th.]: 0.0260
Scan Step Time [s]: 37.9950
Scan Type: Continuous
PSD Mode: Scanning
PSD Length [°2Th.]: 3.35
Offset [°2Th.]: 0.0000
Divergence Slit Type: Fixed
Divergence Slit Size [°]: 1.0000
Specimen Length [mm]: 10.00
Measurement Temperature [°C]: 25.00
Anode Material: Cu
K-Alpha1 [Å]: 1.54060
K-Alpha2 [Å]: 1.54443
K-Beta [Å]: 1.39225
K-A2 / K-A1 Ratio: 0.50000

Generator Settings: 40 mA, 40 Kv

The crystal, chemical composition, and their presence percentage in the samples by the de-vice are given in table 7. The details show that most of the crystals are in the same category. In order to examine more carefully, one from each sample is analyzed qualitatively.

Table 7 . Compositions and percentage of cement crystals

OPC1	H2 Ca1 O2 Portlandite 98-004-6197 36.9%	Ca3 O5 Si1 Hatrurite 98-001-2728 36.4%	Ca2 O4 Si1 Dicalcium Silicate 98-003-6706 24.6%	Mg1 O1 Periclase 98-007-4470 4.2%
OPC2	H2 Ca1 O2 Portlandite 98-004-6197 40.8%	Mg1 O1 Periclase 98-007-4470 4.5%	Ca3 O5 Si1 Hatrurite 98-001-2728 33.2%	Ca2 O4 Si1 Dicalcium Silicate 98-003-6706 21.5%
OPC3	H2 Ca1 O2 Portlandite 98-004-6197 40.9%	Ca3 O5 Si1 Hatrurite 98-001-2728 35.2%	Mg1 O1 Periclase 98-007-4470 4.7%	Ca2 O4 Si1 Dicalcium Silicate 98-003 19.3%
N1	H2 Ca1 O2 Portlandite 98-004-6197 42.1%	Ca3 O5 Si1 Hatrurite 98-001-2728 33.4%	Mg1 O1 Periclase 98-007-4470 4.4%	Ca2 O4 Si1 Dicalcium Silicate 98-003-6706 20.1%
N2	Ca3 O5 Si1 Hatrurite 98-001-2728 33.3%	Ca2 O4 Si1 Dicalcium Silicate 98-003-6706 22.4%	H2 Ca1 O2 Portlandite 98-004-6197 39.6%	Mg1 O1 Periclase 98-007-4470 4.7%
N3	H2 Ca1 O2 Portlandite 98-004-6197 49.5%	Ca3 O5 Si1 Hatrurite 98-001-2728 45.5%	Mg1 O1 Periclase 98-007-4470 5.0%	
M1	H2 Ca1 O2 Portlandite 98-004-6197 34.5%	Ca3 O5 Si1 Hatrurite 98-001-2728 30.1%	Mg1 O1 Periclase 98-003-6706 7.6%	Ca2 O4 Si1 Dicalcium Silicate 98-003-6706 27.9%
M2	H2 Ca1 O2 Portlandite 98-001-7623 39.1%	Ca3 O5 Si1 Hatrurite 98-001-2728 34.2%	Mg1 O1 Periclase 98-007-4470 4.8%	Ca2 O4 Si1 Dicalcium Silicate 98-003-6706 21.9%
M3	H2 Ca1 O2 Portlandite 98-004-6197 38.3%	Ca3 O5 Si1 Hatrurite 98-001-2728 36.8%	Mg1 O1 Periclase 98-007-4470 4.7%	Ca2 O4 Si1 Dicalcium Silicate 98-003-6706 20.2%

Table 8 . Ratio of crystalline phase

sample ID	the sum of the net area	the sum of the total area	crystallinity%
M1	2253.87	22970.43	9.812049666
M2	1726.017	22069.28	7.820903083
M3	1738.32	22031.15	7.890282623
N1	1843.147	24797	7.432943501
N2	1761.05	20298.36	8.675824057
N3	1935.57	25028.08	7.733593628
OPC1	1983.51	28272.99	7.015565032
OPC2	2001.59	23851.35	8.391935886
OPC3	1900.64	24369.66	7.799206062

Table 9 . Comparison of the average ratio of crystalline phase

Group	Ave. crystallinity%	Changes%
M	8.50%	9.96%
N	7.94%	2.72%
OPC	7.73%	

The results demonstrate that the percentage of crystallinity in the samples under the T-Consciousness Field is higher than in the controls; and in sample M, it is significantly higher than in the other two groups. M and N are two different fields. For qualitative evaluation, sample number 2 of each group was selected and analyzed qualitatively since the variations of all three samples from each group are very close to each other.

A qualitative review of the second sample No. 2 of each group

X'Pert Highscore Plus software was used to identify the phase from the results of the X-ray diffraction pattern of these samples. According to Figure 5, it is clear that the main phases are the same in all three samples and the peaks are diffracted at almost the same angles, which indicates that the main compounds are almost the same in all three samples.

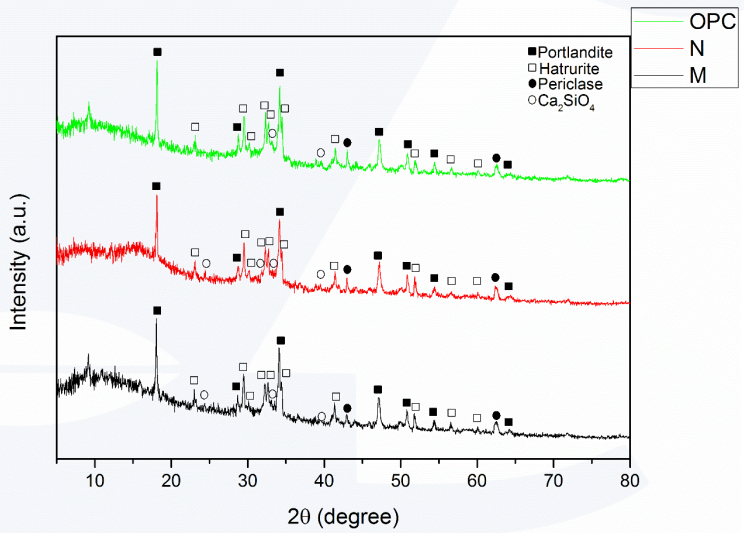

Figure 5. Figure 5- The X-ray diffraction patterns of the hydrated cement samples

According to these diffraction patterns and by matching the visible peaks in these patterns on the reference diffraction patterns by the mentioned software, it was determined that all samples had four phases, which are:

(A) Portlandite phase with the chemical formula Ca (OH)2 and reference code JCPDS No: 98-004-6197 with hexagonal crystal structure and spatial group P-3m1. In this structure, the diffraction plates (001), (100), (101), (102), (110), (111), and (112) are observed at angles of 18.1 °, 28.6 °, 34.1 °, 47.1 °, 50.8 °, 54.3 °, and 64.2 °, respectively.

(B) Harturite phase with chemical formula Ca3SiO5 and reference code JCPDS No: 98-001-2728 with orthorhombic crystal structure and C-E space group. In this structure, the diffraction plates (115), (221), (401), (224), (225), (319), (620), (224) and (629) are observed at angles of 23.1 °, 29.5 °, 30.2 °, 32.3 °, 32.7 °, 34.5 °, 41.4 °, 51.8 °, 59.7 ° and 60.1 °, respectively.

(C) Periclase phase with chemical formula MgO and reference code JCPDS No: 98-007-4470 with cubic crystal structure and space group Fm-3m. In this structure, diffraction plates (200) and (220) are observed at angles of 42.9 ° and 62.3 °, respectively.

(D) Calcium silicate phase with chemical formula Ca_2SiO_4 and reference code JCPDS No: 98-003-6706 with orthorhombic crystal structure and spatial group Pbmn. In this structure, diffraction plates (111), (040), (112), and (211) are observed at angles of 24.4 °, 31.8 °, 33.3 °, and 39.5 °, respectively.

To better compare the intensity of the peaks in each sample, some specified peaks are magnified in the range of specific angles, as shown in Figure 6.

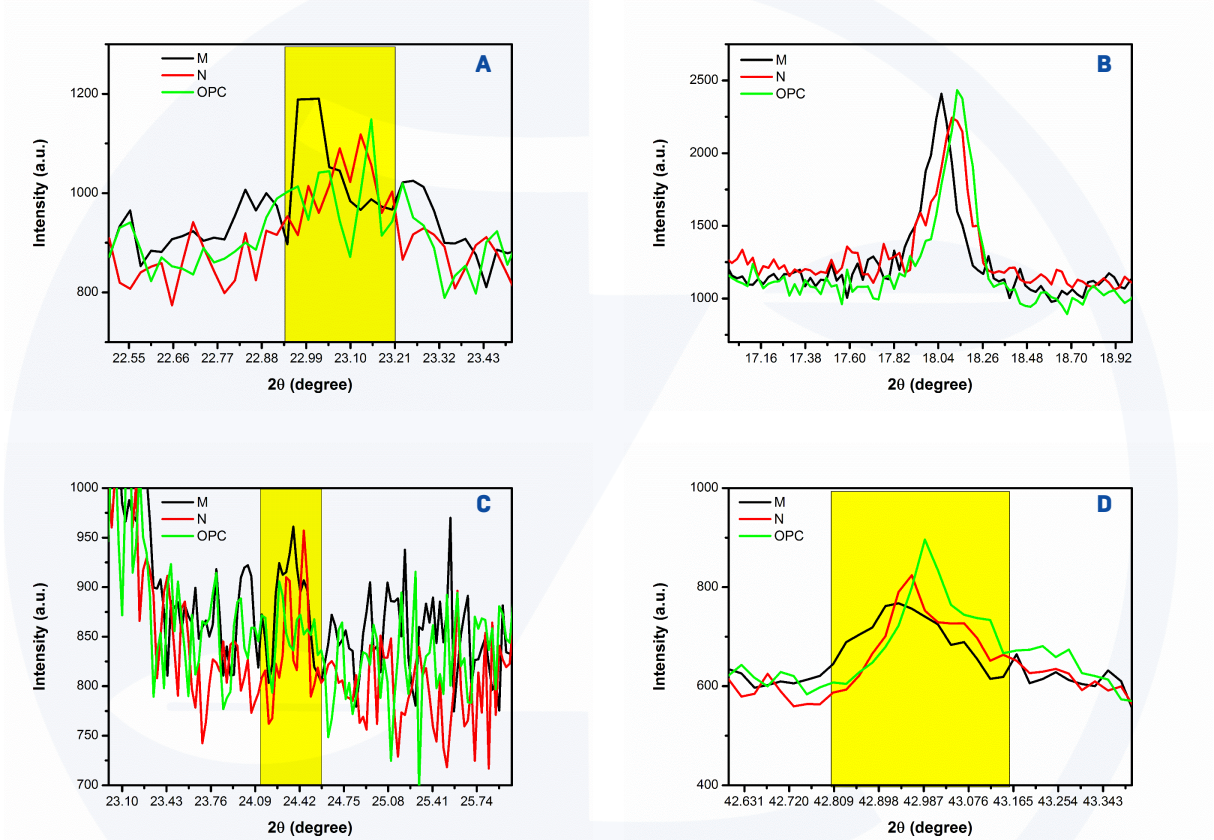

Figure 6. X-ray diffraction patterns were magnified and stacked for peaks related to phases of (a) harturite, (b) portlandite, (c) calcium silicate, and (d) periclase.

According to Figure 6 (A), the harturite phase is almost the same intensity in samples N and OPC, but in sample M the intensity of this peak is higher than in the other two samples. Figure 6 (C) also shows that for the calcium silicate phase, sample M has a relatively higher intensity than the other two samples. The results of the XRF test also show that the CaO phase, which constitutes these two phases, is higher in sample M than in the other two samples. Therefore, it can be concluded from the results that the calcium silicate-based phases, one of which being the harturite phase with the chemical formula Ca_3SiO_5, in sample M are more than the other two samples. In addition, Figure 6 (C), shows that the phase intensity of calcium silicate in the OPC sam-ple is lower than in the other two samples.

In fact, according to the results of the XRF test, it is observed that the amount of SiO_2, which is another compound of the two constituents of calcium silicate, in sample N is

higher than in the other two samples, and it can be concluded that after sample M, sample N has the most silicate phases. Figure 6 (B) shows the peak intensities of the portlandite phase, and it is clear that among the three samples, the peak intensity in sample N is less than in the other two samples. Considering that the results of the XRF test also show that the percentage of CaO in this sample is less than the other two samples, from the results of these two tests, it can be concluded that sample N has less portlandite content than the other two samples.

Figure 6 (D) also shows the intensity of the peaks related to the periclase phase. By comparing the peak intensities, it is clear that the peak intensities in the OPC are higher than the others, followed by the N and M samples. By comparing the MgO values in the XRF test results, the exact order was observed, and therefore it can be concluded that the periclase phase in the OPC sample is more than the other two samples, followed by the N and M samples.

Figure 7 shows that the results of thermal analyses (TGA / DTA / DSC) were carried out for quantitative examination of the compounds of these samples.

Comparison of sample No. 2 of each group and the results of TGA-DTA-DSC analyses

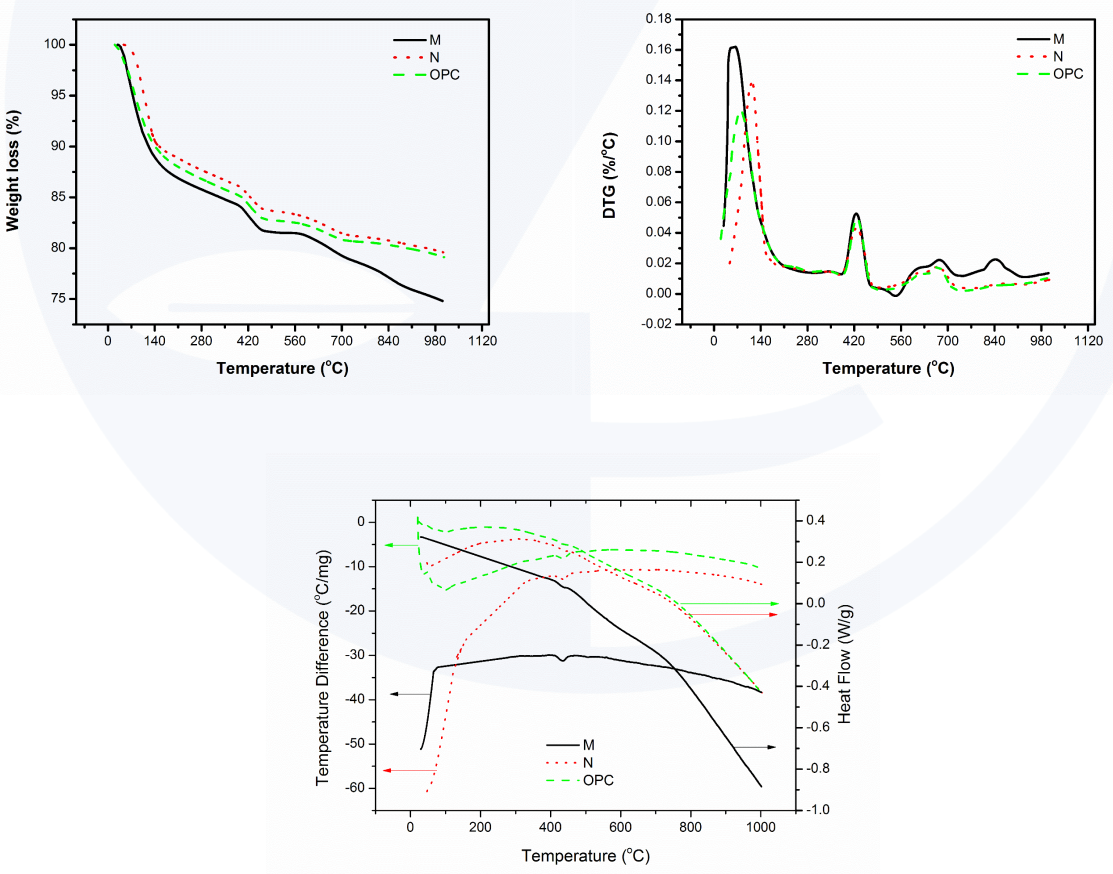

Figure 7. Results of tests (1) TGA, (2) DTG and (3) DTA / DSC on the samples M (TCF), N (TCF), and OPC (Control)

According to Figure 7, Graph (1) shows a weight-loss stage at temperatures below 200 ° C, which is related to the evaporation of structural water and water absorbed in the samples [14]. About 13% of sample M, 12% of sample OPC, and 11% of sample N lost weight in this temperature range. Therefore, it is clear that the difference is small, but it is reasonably meaningful. Considering the importance of the Portlandite phase in water absorption of cement, the lower phase of this phase in sample N than the other two samples, proven in the results of previous tests, can be the most important reason for lower water absorption in this sample. This finding could be the reason for the higher water absorption in sample M because the amount of CaO in the XRF test results was higher than in the other two samples.

The second stage of weight loss, which caused a peak in the DTG diagrams at 420 ° C, and also in the DTA / DSC diagrams, also showed an endothermic peak related to the thermal decomposition of the Portlandite phase [15]. From the intensity of the peaks in the DTG diagrams, it is clear that the value of this phase in all three samples is approximately close to each other. However, the TGA results show that the weight loss in the temperature range of 380 to 490 ° C for the M, N, and OPC samples was about 2.8%, 2.5%, and 2.6%, respectively. The next weight loss stage is in the temperature range of 560 to 700 ° C, which is related to the thermal decomposition of phases based on calcium silicate [16]. The weight reduction of M, N, and OPC samples in this temperature range was about 2.6%, 2.1 and 1.7%, respectively. Sample M has 50%, and sample N has 23% more calcium silicate compared with the control group. This trend is precisely in line with the trend of the values obtained by the results of XRF tests and shows that the silicate phases in samples M and N are more than in the OPC sample.

In addition, in sample M, another weight-loss stage can be observed at a temperature of about 840 °C, which has not been observed in the other two samples of this stage. At this stage, in sample M, about 2.1% of the initial mass of the sample is thermally decomposed. This stage of weight loss is usually related to the calcium carbonate removal from the sample [17], which can be justified by the higher amount of CaO in the XRF test results. Therefore, it can be concluded that in sample M, unlike the other two samples, there is some calcium carbonate.

Conclusion

All results showed that the dimensions of the samples did not change significantly, and the volume remained the same. Regarding the increase in mass, one of the control samples did not show much difference until the age of 7 days, which caused the rate of increase in mass to be 50% higher up to the age of 7 days than the one-day age, the reason for this is not apparent. Then the cement samples enter the hydration process naturally, and the mass changes begin according to Figure (4). The rate of mass growth is 3 to 4% higher in the samples under T-Consciousness Field when their age goes up. According to the results (Tables 5 and 6), the presence of L.O.I in the Control is more than in the TCF. This implies that the weight change is not dependent on water absorption and light elements. From the XRD results (Tables 7 and 8), it is clear that the chemical compounds are composed of different percentages, and the percentage of crystalline phases is higher in the samples under the TCF (Tables 9).

There was about ~10% more crystalline phase in sample M than in the control group.

As can be seen from the image of this sample, the pulverized cement also had a different tex-ture and color (Figure 3). The thermal analy-sis (Figure 7) shows that the lost water in the samples is not significant, and the differences depen d on the changes in matter. Sample M has 50%, and sample N has 23% more calcium silicate compared with the control group. In sample M, unlike the other two

samples, there is some calcium carbonate. These changes can be examined from two perspectives. First, the cement hardening process has been so that under the T-Consciousness Fields, the tendency to absorb less water and to create denser compounds in it has intensified.
Second, according to the results of the XRF, which show a repetitive pattern in the samples, as seen in the other studies, the cement elements have changed in addition to low water absorption. That is, the composition of the cement substance has changed, and then the chemical reactions have also changed.

This possibility is debatable since the primary cement, and all conditions were the same in this experiment. The difference in water absorption in the samples under the T-Consciousness Field is almost zero. However, their constituent elements' type and weight percentage are different after hydration. For example, Na is not reported in any M group samples. Aluminum or phosphorus, for example, reports the same change pattern, which is almost repetitive. This implies a conversion between T-Consciousness, matter and energy. Not only are the reactivities different, but the degree of presence of the elements has also changed under the T-Consciousness in a different way. Obviously, not all cement elements can be obtained exactly, but given the process of these changes in other research on cement, the results of both probabilities are reported.

From t he results of extensive changes in the behavior and structure of various materials, i t is concluded that T-Consciousness, according to Taheri's theory, can be converted into matter and energy [1, 2].

T-Consciousness ↔ Wave (Matter and Energy)

References

1. Taheri, M. A. (2020). The main monitoring center for T-Consciousness Fields research and studies based on Sciencefact. www.Cosmointel.com.
2. Taheri, M. A. (2012). General Connection of Particles. Interuniversal Publishing Erfan-Halgheh. ID: 978-1-940491-03-5.
3. Taheri, M. A. (2013). Human from Another Outlook (2nd Edition). ISBN-13: 978-1939507006, ISBN- 10: 1939507006.
4. Kazazi, B, & Taheri, M. A. (2021). Effect of the Consciousness Bond Field on the structure and properties of Aluminum. Retrieved from www.cosmointel.com.
5. Kazazi. B, & Taheri. M. A. (2021). Effect of the Consciousness Bond Field on the structure and properties of 1000- series Auminum with preheating Retrieved from www.cosmointel.com.
6. Rawdon H.R., Krynitski A.I., Berliner J.F., Brittleness developed in aluminium and duralumin by stress and corrosion, Chemical Metallurgy Engineering, vol. 26 (1922), p. 154–160.
7. Kazazi. B, & Taheri. M. A. (2021). Study of density changes and increase in the length of pure copper up to 300 °C in Consciousness Bond Field. Retrieved from www.cosmointel.com.
8. Kazazi. B, & Taheri. M. A. (2021). Study of the effect of the Consciousness Bond Field on mechanical crushing of silica particles preheating Retrieved from www.cosmointel.com.
9. Kazazi. B, & Taheri. M. A. (2021). Influence of Consciousness Bond Field on the plant synthesis of nano-silver preheating Retrieved from www.cosmointel.com.
10. Kazazi, B., & Taheri, M. A. (2021). Influence of Consciousness Bond Field (CF) on crystallization and strength of cement mortar (concrete). Retrieved from www.cosmointel.com.
11. Kazazi, B., & Taheri, M. A. (forthcoming 2022). Comparison of the behavior of concrete made under the influence of Taheri Consciousness Fields (TCFs), and under gamma and neutron radiations, with ordinary concrete, when receiving TCF and gamma and neutron radiations simultaneously.
12. Kazazi, B., & Taheri, M. A. (forthcoming 2022). Investigation of chlorine ion penetration in concrete under the influence of Taheri Consciousness Fields.
13. Kazazi, B., & Taheri, M. A. (2021). Effects of the T-Consciousness Field on Concrete (ASR. Retrieved from www.cosmointel.com.
14. Soares.L.W.O, R.M. Braga, J.C.O. Freitas, R.A. Ventura, D.S.S. Pereira, D.M.A. Melo,.(2015). The effect of rice husk ash as pozzolan in addition to cement Portland class G for oil well cementing, Journal of Petroleum Science and Engineering. 131 - 80–85. doi:10.1016/j.petrol.2015.04.009.
15. Sharma.D.K , Sharma.R,.(2018). Influence of rice husk ash and rice tiller ash along with chromate reducing agents on strength and hydration properties of Ordinary Portland Cement, Construction and Building Materials. 169 - 843–850. doi:10.1016/j.conbuildmat.2018.03.044.
16. Tantawy.M.A , Shatat.M.R, El-Roudi.A.M , Taher.M.A, Abd-El-Hamed.M ,.(2014). Low Temperature Synthesis of Belite Cement Based on Silica Fume and Lime, International Scholarly Research Notices. 1–10. doi:10.1155/2014/873215.
17. Sabeur.H , Saillio.M, Vincent.J ,.(2019). Thermal stability and microstructural changes in 5 years aged cement paste subjected to high temperature plateaus up to 1000 °C as studied by thermal analysis and X-ray diffraction, Heat and Mass Transfer. 55 - 2483–2501. doi:10.1007/s00231-019-02599-w.